



MINISTERIO DA CIENCIA E TECNOLOGIA

INSTITUTO DE PESQUISAS ESPACIAIS

BR 881E98G

8. Title *INPE-4150-PH/1081*

*EXPERIMENTAL MODEL OF HALO PLASMA OBSERVED
IN SMALL-ASPECT ARC PLASMA*

9. Authorship *Yoshiyuki Aeo*

Responsible author

Yoshiyuki Aeo

1. Publication NO INPE-4159-PRE/1061	2. Version	3. Date April 1987	5. Distribution <input type="checkbox"/> Internal <input checked="" type="checkbox"/> External <input type="checkbox"/> Restricted
4. Origin IAP	Program FMAG		
6. Key words - selected by the author(s) PLASMA PHYSICS HALO PLASMA MAGNETIC FIELD PLASMA CONFINEMENT FIELD REVERSED CONFIGURATION			
7. U.D.C.: 533.9			
8. Title INPE-4159-PRE/1061 EXPERIMENTAL MODEL OF HALO PLASMA OBSERVED IN SMALL-ASPECT FRC PLASMA		10. NO of pages: 35	11. Last page: 25
9. Authorship Yoshiyuki Aso		12. Revised by <i>B. H. ...</i> José Augusto Pittelcourt	
Responsible author <i>Yoshiyuki Aso</i>		13. Authorized by <i>[Signature]</i> Marco Antonio Rangel Director General	
14. Abstract/Notes The halo plasma, which is a thin plasma surrounding the Field Reversed Configuration (FRC), was observed in the Staged Theta Pinch-linear (STP-L) experiment. The experimental results show that the ion flow in the halo plasma increases in opposite directions at the vicinity of the separatrix and at the edge of the halo, when the end effect is reduced by the guide field. This double structure of ion flow may be explained by the proposed model that the halo plasma is formed by energetic ions shuttling between the FRC and the open field region, and the numerical result is in good agreement with the experiment. The proposed model also suggests that the FRC has a good confinement ability for the energetic particles if the plasma does not connect with the discharge tube.			
15. Remarks To be admitted for publication in Nuclear Fusion.			

EXPERIMENTAL MODEL OF HALO PLASMA OBSERVED IN SMALL ASPECT FRC PLASMA

YOSHIYUKI ASO

Laboratório Associado de Plasmas - LAP

Instituto de Pesquisas Espaciais - INPE

12225 - São José dos Campos, SP

Brazil

ABSTRACT. The halo plasma which is a thin plasma surrounding the Field Reversed Configuration (FRC), was observed in the Staged Theta Pinch-linear (STP-L) experiment. The experimental results show that the ion flow in the halo plasma increases in opposite directions at the vicinity of the separatrix and at the edge of the halo, when the end effect is reduced by the guide field. This double structure of ion flow may be explained by the proposed model that the halo plasma is formed by energetic ions shuttling between the FRC and the open field region, and the numerical result is in a good agreement with the experiment. The proposed model also suggests that the FRC has a good confinement ability for the energetic particles if the plasma does not connect with the discharge tube.

1. INTRODUCTION

It was observed in the Staged Theta Pinch-Linear (STP-L) experiment in Nagoya University [1] that the Field Reversed Configuration (FRC) plasma has a thin plasma surrounding it which is called, here, "halo plasma", although such a halo plasma is not clearly observed in other FRC experimental devices. This difference seems to be characterized by the parameter r_s/ρ_i , where r_s is a separatrix radius of the FRC and ρ_i is the ion Larmor radius for the vacuum magnetic field. In the case of STP-L, $r_s/\rho_i \sim 3$, but in other experimental devices, for example FRX-A, B [2] and C [3], PIACE [4], NUCTE [5] and so on, $r_s/\rho_i \geq 5$. A plasma with $r_s/\rho_i < 5$ is defined, here, as a "small-aspect" plasma.

The halo plasma has not been investigated because the plasma is very thin and was not clear in many experimental devices. In the STP-L experiment, however, the halo plasma surrounding the FRC was clearly observed, and its plasma rotation was firstly measured [1, 6]. The experimental results show that the behavior of the halo plasma is closely related to the rotation of the FRC plasma, and also shows that, when the plasma touched the wall of the discharge tube at the end of the coil, its effect, which is called in general "end effect", appears first in the halo plasma [7]. From these results, it can be said that the halo plasma may be of importance since it receives the effect from both the outer and inner regions. Namely, by examining the behavior of the halo plasma, some information about the FRC plasma may be obtained, without disturbing the FRC itself.

The STP-L experiment was done by reducing the end effect, so that the outer and inner effects could be separated for the first time. From this experiment, the following results were found: by reducing the end effect, (1) the rotational instability can be stabilized [1], (2) the rotation of the FRC plasma is decelerated [6, 8], and (3) the double structure of ion flow in the halo plasma is observed [6]. The present work is devoted to the examination of phenomenon (3). Section II describes the experimental results on the ion flow in the halo plasma. In Section III, an experimental model is proposed to explain the double structure of ion flow in the halo plasma. Under this model the motion of the particles forming the halo plasma is calculated in Section IV, and is compared with the experimental results. In Section V, the rotation and confinement of the FRC plasma are discussed, and the conclusions of this paper are summarized.

11. EXPERIMENTAL RESULTS

The STP-L apparatus, the schematic drawing of which is shown in Fig. 1(a), has two unique features, i.e., the guide field coils, 2.7m long, attached to both ends of the main θ -pinch coil, and the fast-acting gas valves to inject the working gas into the discharge tube. The guide coils generate a quasi-static uniform axial field of 0.5T, by which the plasma ejected from the main coil is guided out to the ends of the apparatus. The main coil, 1.5m long and with an inner bore of 12cm, is excited by the super-fast and the fast banks, which generate an axial field of 0.25T and 1T, with rise-times of 0.2 μ s and 2.4 μ s, respectively. The strength of the quasi-static negative bias field is 5.5×10^{-2} T. The time evolution of these fields are shown in Fig. 1(b). The working D_2 gas is puffed at the center of the main coil by two specially designed fast-acting gas valves whose muzzles also serve as electrodes for the small coaxial plasma guns. Therefore, its density distribution along the axis is of a transient character. Thus, the volume-averaged gas pressure is employed here as a measure of the filling-gas density; it was chosen to be 8.6mTorr in this experiment. The main discharge is always fired when the expanding gas fronts reach the ends of the main coil. Therefore, we may expect that the hot plasma created in the main coil expands into the vacuum along the guide field (GF) up to the ends of the apparatus, and that the end effect is eliminated until the plasma tips hit the end wall.

Actually, it is observed that the end effect is delayed for about 14 μ s after implosion by the GF [7], which means that the onset time of a rotational instability in the FRC plasma is also delayed, as shown in

Fig. 2. Excluded-flux measurement shows that the edge of the bright core in Fig. 2 corresponds to the separatrix of the FRC, so that the halo plasma observed around the bright core should be in the open field region. The relative ion current in the open field region is measured by the directional probe [9] shown in Fig. 3(a). The ion current is obtained from the difference between the measurements in two opposite directions 1 and 2, as shown in Fig. 3(b). The reproducibility in each measurement is confirmed with 3-4 shots of the discharge. These data, measured for the two cases with and without the GF, are shown in Fig. 4. It is mentioned here that the separatrix radius r_s is about 1.8cm and its surrounding halo plasma in the open field region has a radius of about 3.0cm, which are measured by the streak photographs. From Fig. 4 it is noticed that, in the case with GF, (1) the direction of ion current near the separatrix ($r \sim 2.0$ cm) reverses about $5\mu s$ after implosion, in contrast with the case without GF, and its direction is the same as that of the electron diamagnetic current, and (2) the ion current around the edge of the halo plasma ($r \sim 3$ cm) has the peak value in the direction of the ion diamagnetic current in opposite sense to the current near the separatrix, while in the case without GF it does not change particularly. The time behavior of the ion current at $r = 2.0$ cm and $r = 2.5$ cm, $14\mu s$ after implosion in the case with GF, is similar to the case without GF. These can be regarded as the same phenomena caused by the end effect, because the plasma in the case with GF is left under the condition connected with the wall of the discharge tube after about $14\mu s$. Consequently, the double structure of ion flow in the halo plasma, which has occurred $14\mu s$ earlier in the case with GF, is independent of the end effect, and should arise from the character of the plasma itself.

For this phenomenon an experimental model is proposed in the next section, and the model results are compared with the experimental results.

III. EXPERIMENTAL MODEL OF THE HALO PLASMA

The origin of the halo plasma may be due to one of the following three cases: (1) a plasma left in the formation phase of the FRC; (2) a diffused plasma from the inside of the FRC after the formation; and (3) a plasma connecting with the FRC plasma. The experimental result that $r_s/\rho_i \sim 3$ is inconsistent with cases (1) and (2) for the halo plasma. In this paper we consider therefore the plasma in case (3), which is floating across the vacuum magnetic field, and is independent of the end effect.

The plasma parameters collaborate on the conclusion that the halo plasma is produced from particles being shuttled from the FRC to the open field region. Table 1 shows the plasma parameters in this experiment, and the basic quantities of the FRC plasma, estimated from Table 1, are shown in Table 2. In these quantities it is noticed that the ion Larmor radius ρ_i is comparable with the minor radius a of the FRC ($\rho_i \sim a$), while the electron Larmor radius is much smaller ($\rho_e \ll a$), and also that these particles are almost in a collisionless situation ($\omega_i \tau_{ij} \gg 1$ and $\omega_e \tau_{ei} \gg 1$). Since the FRC has a null point ($B = 0$) inside it, some of the ions at the null point can easily come out from the FRC, under the above condition. These particles form the halo plasma.

The behavior of the halo plasma will be considered, here, under the following assumptions:

- (1) The magnetic field configuration of the FRC is given explicitly.
- (2) The temperature of confined ions is isotropic on the null point ($B = 0$ at $r = r_0$) inside the FRC.

(3) All confined ions pass through the null point, and can move freely along their Larmor orbits.

(4) All electrons are frozen in the magnetic field, and provide the quasi-neutrality for the ion motion with large Larmor radius.

(5) The FRC plasma rotates as a rigid body.

Assumption (1) is consistent with the experimental result that the diameter of the FRC is almost constant after implosion. Assumption (2) is also consistent with the experiment [10]. The assumption (3) may be reasonable from a point of view of the small-aspect FRC plasma ($\rho_i \sim a$). For assumption (4), the following reason is given: since the particle confinement in the open field region is much poor than the one in the closed field region, the density gradient on the separatrix surface becomes steep. In this experiment the characteristic density gradient length δ_n is comparable with the minor radius a of the FRC. The growth rate of microinstability caused by the ion motion with large Larmor radius ρ_i , then, becomes largest for the lower hybrid drift instability [11], the saturation growth time of which is less than 10ns under the experimental conditions of $\rho_i/2\delta_n \sim 0.5$ and $\omega_{LH} \sim 1.7 \times 10^9 \text{ s}^{-1}$. Consequently, these microinstabilities may be saturated in the ion Larmor period of about 200ns in the present case, in which time the electrons can be scattered along the Larmor orbit.

The assumption (5) is equivalent to that the equiflux surface corresponds to the equipotential surface inside the FRC. One of the characteristic features of the FRC is the presence of the null point in the magnetic field, which is wrapped up only in a poloidal magnetic field. Therefore, each line of force between the coil axis and the null

point (magnetic axis) must pair with that between the null point and the separatrix. In other words, the different flux surfaces are isolated from each other. In such a FRC, rotating with the azimuthal velocity \vec{V}_f , the plasma feels an electric field \vec{E}' , given by

$$\vec{E}' = \vec{V}_f \times \vec{B} . \quad (1)$$

Since each equiflux surface is isolated, an electrostatic field \vec{E} is created in the opposite direction to \vec{E}' ,

$$\vec{E} = -\vec{V}_f \times \vec{B} . \quad (2)$$

In cylindrical coordinates, Eq. (2) becomes

$$\vec{E} = -\frac{V_f \theta}{r} \frac{\partial \psi}{\partial r} \vec{e}_r - \frac{V_f \theta}{r} \frac{\partial \psi}{\partial z} \vec{e}_z , \quad (3)$$

where ψ is a flux function such that $\psi = rA\theta$. From the relation $\vec{E} = -\vec{\nabla}\phi$, we have

$$\frac{\partial \phi}{\partial r} = \frac{V_f \theta}{r} \frac{\partial \psi}{\partial r}$$

and

$$\frac{\partial \phi}{\partial z} = \frac{V_f \theta}{r} \frac{\partial \psi}{\partial z} . \quad (4)$$

Here, taking account of the condition that the equipotential surface is equivalent to the equipotential surface, i.e., $\phi \propto \psi$, we get one of the solutions for $V_{f\theta}$ as follows,

$$V_{f\theta} = r\Omega, \quad (5)$$

where Ω is the rigid body angular velocity of the FRC plasma, independent of r and z . If the potential on the separatrix surface is zero, then the relation of ϕ and ψ becomes

$$\phi(r,z) = \psi(r,z). \quad (6)$$

It is noticed, here, that the rotation of the FRC plasma is free as for a rigid body rotation about the axis.

IV. PARTICLE MOTION FROM THE INSIDE OF THE FRC

In the preceding section, it is proposed that the halo plasma surrounding the small aspect FRC is generated by particles being shuttled from the inside of the FRC to the open field region. The interesting problem here is how particles come out from the FRC under the action of the radial electric field. We consider this problem only for the radial dependency of the confined particles, from the point of view of the confinement capability perpendicular to the magnetic field.

In cylindrical coordinates, the equation of motion to be solved is as follows:

$$m(\ddot{r} - r\dot{\theta}^2) = qEr + q\dot{\theta} \frac{d\psi}{dr}$$

and

(7)

$$m(r\ddot{\theta} + 2\dot{r}\dot{\theta}) = -q \frac{\dot{r}}{r} \frac{d\psi}{dr}$$

where q is the ion charge, m is the ion mass, and E_r is a radial electric field inside the FRC given by $E_r = -\Omega \frac{d\psi}{dr}$, from Eq. (6). Because of this electric field, the FRC plasma rotates about the axis. Thus, we rewrite Eq. (7) using a rotating cylindrical coordinate system (r', θ') with the constant angular velocity Ω , as follows:

$$m\ddot{r}' = mr'(\dot{\theta}' - \Omega)^2 + q(\dot{\theta}' - \Omega) \frac{d\psi}{dr} - q\Omega \frac{d\psi}{dr} \quad (8)$$

and

$$mr'^2(\dot{\theta}' - \Omega) + q\psi = \text{const.} , \quad (9)$$

where $r = r'$ and $\theta = \theta' - \Omega t$. On the right hand side of Eq. (8), the first and the second terms are the centrifugal force and the Lorentz force (due to the magnetic field) terms, respectively, and the third one is the electric field produced by the rotation of the bulk plasma. For convenience, we replace here r' and θ' by r and θ , respectively, so that after some algebra we obtain the following equations for the radial (v_r) and the azimuthal (v_θ) velocities:

$$v_r^2 = v_{r_0}^2 + \left(1 - \frac{r_s^2}{2r^2}\right) \left\{ v_{\theta_0} - \frac{r_s}{\sqrt{2}} \Omega + \sqrt{2} r_s \frac{\frac{q}{m}(\psi - \psi_0)}{2r^2 - r_s^2} \right\}^2 - \frac{q^2(\psi - \psi_0)^2}{m^2 r^2} \left(1 + \frac{r_s^2}{2r^2 - r_s^2}\right) - \frac{2q}{m} (\psi - \psi_0) \Omega \quad (10)$$

and

$$v_\theta = \frac{v_{\theta_0}}{\sqrt{2}} + \frac{r_s}{r} - \frac{q}{mr} (\psi - \psi_0) + \frac{\Omega}{2r} (2r^2 - r_s^2) , \quad (11)$$

where ψ_0 , V_{r_0} and V_{θ_0} are the flux function, line radial and the azimuthal velocities at the field null point, respectively.

The particles which are confined inside the FRC and which satisfy the condition that $V_r^2 < 0$ on the separatrix surface are described in the velocity space by the following inequality:

$$V_{r_0}^{*2} + \frac{1}{2} \left(V_{\theta_0}^* - \frac{1}{\sqrt{2}} \Omega^* - \sqrt{2} \psi_0^* \right)^2 < 2\psi_0^* - 2\psi_0^* \Omega^* . \quad (12)$$

This equation is normalized by the quantity $\omega_i^2 r_s^2$. Thus, $V_{r_0}^* = V_{r_0} / \omega_i r_s$, $V_{\theta_0}^* = V_{\theta_0} / \omega_i r_s$, $\Omega^* = \Omega / \omega_i$ and $\psi_0^* = \psi_0 / B_e r_s^2$, where ω_i is the ion cyclotron angular frequency for the external field B_e . The absolute confinement region in the FRC described by Eq. (12) is then bounded by an ellipse curve centered off the origin in velocity space, and its position and size depend on the angular velocity Ω^* of the FRC plasma, as shown in Fig. 5. For this asymmetric confinement region, it is noticed that the isotropic plasma on the null point spreads symmetrically around the origin ($V_{r_0}^* = V_{\theta_0}^* = 0$) with a Maxwellian distribution. This means that the number of particles, other than the absolutely confined ones, which are in the incomplete confinement region in Fig. 5, is strongly dependent on the angular velocity of the FRC plasma. These particles form the halo plasma. Consequently, the behavior of the halo plasma depends on the rotation of the FRC plasma.

It must be mentioned here that the FRC plasma can rotate freely as a bulk, but the rotation of the plasma in the open field region is complicated because the flux surface is open. For the calculation of ion flow in the open field region, the effect of the FRC plasma rotation is

examined here. The ion distribution function on the null point inside the FRC is a Maxwellian one, of the form

$$f = \frac{n_0}{\pi} \cdot \frac{r_s^2}{\rho_i^2} \exp \left\{ - \frac{r_s^2}{\rho_i^2} (v_{r_0}^{*2} + v_{\theta_0}^{*2}) \right\}, \quad (13)$$

where n_0 is the number of particles per unit volume, and ρ_i is the ion Larmor radius. When an ion reaches the separatrix surface, it has the following radial v_{rs}^* and azimuthal $v_{\theta s}^*$ velocity components:

$$v_{rs}^{*2} = v_{r_0}^{*2} - \frac{1}{2} \left(v_{\theta_0}^* - \frac{\Omega^*}{\sqrt{2}} - \sqrt{2}\psi_0^* \right)^2 - 2\psi_0^{*2} + 2\psi_0^*\Omega^* \quad (14)$$

and

$$v_{\theta s}^* = \frac{v_{\theta_0}^*}{\sqrt{2}} + \psi_0^* + \frac{3}{2}\Omega^*. \quad (15)$$

With these velocity components, the ion is shot from the rotating FRC plasma into the open field region. From this initial velocity and the equation of motion, we can calculate the ion current in the open field region. Figure 6 shows the numerical result for the ion current integrated over the distribution function of Eq. (13). The ion current is normalized by the quantity $2n_0\omega_i r_s$, and Hill's vortex is assumed for the flux function, so that $\psi_0^* = -1/8$. It is noticed here that the current evolution as a function of Ω^* is similar to the experimental result of the directional probe in the case with the guide field (see Fig. 4) up

to $14\mu\text{s}$ after implosion, although the quantities on the horizontal axes are different. The experiment with guide field shows that until about $14\mu\text{s}$ after implosion the plasma is floating across the vacuum magnetic field, which means that the plasma is isolated. So, it can be thought that, due to the loss of ion particles with large Larmor radius, the radial electric field which corresponds to $E_r = -\Omega \partial\phi/\partial r$, is built up with time. If we take the experimental parameters $B_e = 6\text{kG}$ and $r_s = 1.8\text{cm}$, the value $\Omega^* = 0.2$ corresponds to a rotational velocity of $5.8 \times 10^6 \text{rad/sec}$. Thus, the above electric field becomes $-6.3 \times 10^4 \text{V/m}$ at the inner separatrix surface, which also corresponds to a potential well of -140V . Such an electric potential is not still confirmed experimentally, but it is essential in the present model to explain the double structure of ion flow in the halo plasma. On the other hand, the value of ion current becomes about $-3 \times 10^5 \text{A/m}^2$ when $I^* = -2.5 \times 10^{-21}$ at $\Omega^* = 0.2$ and $n_0 \sim 10^{21} \text{m}^{-3}$. This value is roughly in agreement with the experimental value of $-1.8 \times 10^6 \text{A/m}^2$ at $14\mu\text{s}$.

The physical picture of this halo plasma, which is shown in Fig. 7, is as follows. Due to the increase of the radial electric field caused by ion loss, the particle rotation in the direction of the electron diamagnetic current (the positive flow particle) is increased, which also corresponds to the increase of the absolute confinement region in velocity space (see Fig. 5). At the vicinity of the separatrix surface, the positive flow also increases. As a result of Larmor motion the negative flow at the position of $2\rho_i$ off separatrix increases. If we consider the end effect for the above process, the end effect can be regarded as the opposite process, so that the radial electric field

decreases, which means that the absolute confinement region in velocity space decreases toward the vanishing point.

V. DISCUSSION AND CONCLUSION

The double structure of ion flow in the halo plasma observed in the STP-L experiment is explained through the proposed model that the halo plasma is formed by particles being shuttled between the outside and inside of the FRC. The FRC plasma in the present experiment is confined to a magnetic configuration of small scale comparable to the ion Larmor radius. Such a configuration has a very asymmetric confinement region in velocity space as shown in Fig. 5. If the FRC is of large scale relative to the Larmor radius of the confined particle, i.e. $r_s/\rho_i > 5$, the effect of the asymmetric configuration may be neglected, as is the case for the electron in Fig. 5. In the small aspect FRC, however, the asymmetric character is not negligible in a point of view that the particles rotating in the direction of the ion diamagnetic current ($v_\theta < 0$) can be more confined than the particles with velocity $v_\theta > 0$. This means that the particles confined to the FRC begin to rotate naturally in the direction of negative v_θ . Because of this contradiction, the radial electric field was introduced to explain the behavior of ion flow in the halo plasma. As shown in Fig. 5, when the direction of the radial electric field is inward ($\Omega^* > 0$), the FRC plasma confinement is improved, and when it is outward ($\Omega^* < 0$) the confinement region decreases, whose results might be caused by the end effect. It is mentioned here that this rotation is the bulk rotation in the direction of the electron diamagnetic current for the case $\Omega^* > 0$ and is due to the electrostatic field caused by the loss of ions. Such an electric field is special not only for the FRC, but was always observed in a Tokamak plasma [12, 13], which is the toroidal plasma without the end

effect, and also the poloidal rotation by the electric field was observed [13]. In the case of the FRC, this rotation corresponds to the toroidal rotation, and the inverse rotation (to the ion sense) observed in the early phase of the discharge in the STP-1 experiment [8] might correspond to that rotation.

The inward electric field caused by the ion loss produces initially the electron rotation in the direction of the electron diamagnetic current. This electron rotation also produces the induced electric field E_{θ} , which accelerates the ions in the same direction of $\Omega^* > 0$, leading to the bulk rotation. Since the electron current forms the diamagnetic current, in the case of the Tokamak, this current decreases the magnetic pressure in its inner region, but in the FRC it increases the inner magnetic field, because the magnetic field in the inner region of the FRC reverses. Thus, there are two rotations in the FRC plasmas: one is the bulk rotation related to Ω^* and the other is a particle rotation related to $v_{\theta_0}^*$, as shown in Fig. 5, and the particles coming out from the FRC have the two information, which may be measured by the directional probe.

As a conclusion, the double structure of ion flow in the halo plasma may be regarded as one of the phenomena in the process for the FRC to change from the asymmetric confinement configuration to the symmetric one, considering the isolated system. This phenomenon is due to the reversal of inner and outer magnetic field lines in the confinement region, and if the field does not reverse, for example, Tokamak and so on, the confinement character will change for the worse because of the higher energy particles. Since the above characteristic of FRC implies

in particle loss, the supply of particles will be important for the FRC. It is mentioned finally that the condition in the present experiment ($r_s/\rho_i < 5$) may be similar to that of the α -particle confinement in the fusion plasma.

ACKNOWLEDGEMENTS

The author would like to acknowledge Dr. J.A. Bittencourt for reading the manuscript.

REFERENCES

- [1] ASO, Y., WU, Ch., HIMENO, S., HIRANO, K., End Effects on the $n = 2$ Rotational Instability in the Reversed-Field Theta-Pinch, Nucl. Fusion 22 (1982) 843.
- [2] ARMSTRONG, W.T., LINFORD, R.K., LIPSON, J., PLATTS, D.A., SHERWOOD, E.G., Phys. Fluids 24 (1981) 2068.
- [3] SIEMON, R.E., The FRX-C Staff, in Compact Toroids Workshop (Proc. 4th US-Japan Workshop on Compact Toroids, Osaka and Nagoya, 1982), Osaka and Nagoya Universities (1982). 122.
- [4] OHI, S., OKADA, S., TANJYO, M., MINATO, T., ITO, Y., ISHIMURA, T., ITO, H., in Compact Toroids (Proc. US-Japan Workshop, Osaka, 1981), Osaka University (1981) 11.
- [5] NOGI, Y., SHIMAMURA, S., OGURA, H., OSANAI, Y., SAITO, K., YOKOYAMA, K., SHIINA, S., HAMADA, S., YOSHIMURA, H., MAEJIMA, Y., *ibid.*, 29.
- [6] ASO, Y., Experimental Study on Rotation of Field Reversed Configuration Plasma (in Japanese), PhD Thesis, Nagoya University (1984).
- [7] ASO, Y., HIRANO, K., Plasma Behavior in the Open Field Region of Reversed-Field Theta-Pinch, J. Phys. Soc. Japan. 52 (1983) 1095.

- [8] MINATO, T., TANJO, M., OKADA, S., ITO, Y., KAKO, M., OHI, S., GOTO, S., ISHIMURA, T., ITO, H., NOGI, Y., SHIMAMURA, S., OSANAI, Y., SAITO, K., YOKOYAMA, K., SHIINA, S., HAMADA, S., YOSHIMURA, H., ASO, Y., WU, Ch., HIMENO, S., OKAMOTO, M., HIRANO, K., Plasma Physics and Controlled Nuclear Fusion Research (Proc. 9th Int. Conf. Baltimore, 1982) IAEA-CN-41/M-3, IAEA, Vienna.
- [9] BENGTSON, R.D., ECKSTRAND, S.A., SGRO, A.G., NIELSON, C.W., Phys. Rev. Lett. 39 (1977) 884.
- [10] ASC, Y., HIMENO, S., HIRANO, K., Experimental Studies on Energy Transport in a Reversed-Field Theta-Pinch, Nucl. Fusion 23 (1983) 751.
- [11] DAVIDSON, R.C., KRALL, N.A., Nucl. Fusion 17 (1977) 1313.
- [12] HALLOCK, G.A., MATHEW, J., JENNINGS, W.C., HICKOK, R.L., WOOTTON, A.J., ISLER, R.C., Phys. Rev. Lett. 56 (1986) 1248.
- [13] BUGARYA, V.I., GORSHKOV, A.V., GRASHIN, S.A., IVANOV, I.V., KRUPIN, V.A., MEL'NIKOV, A.V., RAZUMOVA, K., SOKOLOV, Yu.A., TRUKHIN, V.M., CHAIKIN, A.V., YUSHMANOV, P.N., KRUPNIK, L.I., NEDZEL'SKIJ, I.S., Nucl. Fusion 25 (1985) 1707.

FIGURE CAPTIONS

Fig. 1 - (a) Schematic drawing of STP-L apparatus.

(b) Time evolution of the main B_z and B_{GF} magnetic fields.

Fig. 2 - Side-on streak photographs with and without guide field. The central bright core corresponds to the FRC plasma, and its surrounding thin image is the halo plasma.

Fig. 3 - (a) Schematic drawing of directional probe.

(b) Two directions on the probe measurement. The ion current was measured by cancelling the electron current in the two direction measurements.

Fig. 4 - Ion currents in the open field region measured by the directional probe. The positive ion current corresponds to the ion flow in the direction of the ion diamagnetic current.

Fig. 5 - (a) Variable particle confinement region of FRC in the velocity phase space. Ω^* is angular velocity of FRC plasma as a rigid body, which is normalized by the ion Larmor frequency of ω_i . ψ_0^* is the trapped flux inside the FRC, which is also normalized by $r_s^2 E_e$. Through the relation of $\psi_0^* = -\frac{1}{8}$, the Hill's vortex is assumed for the magnetic field profile. The dotted parabolic curve is a trajectory of the semiminor radius of ellipse curve for Ω^* . The direction of positive $v_{\theta_0}^*$ is in the electron sense, which is contrary to the experimental data in Fig. 4.

(b) Ion and electron distribution functions estimated from the experimental data for $r_s/\rho_i \sim 3.7$ and $r_s/\rho_e \sim 390$, respectively.

Fig. 6 - Ion current evolutions in the halo region for the rigid angular velocity Ω^* of the FRC, where $I^* = I_{ion}/2n_0\omega_i r_s$. The positive direction of the vertical axis is in the direction of the ion diamagnetic current which is the same as the experimental result of Fig. 4.

Fig. 7 - Physical picture of the halo plasma flow.

TABLE CAPTIONS

Table 1 - Parameters of the FRC plasma in the STP-L experiment.

Table 2 - Basic quantities of the FRC plasma in the STP-L experiment.

quasistatic phase	4 μ s to 16 μ s		unit
B_e : external field	8.0	5.5	kG
T_i : ion temperature	350	200	eV
T_e : electron temperature	120		eV
\bar{n}_e : average electron density	5.5×10^{15}	4.0×10^{15}	cm^{-3}
r_s : separatrix radius	18	15	mm
r_0 : major radius ($\equiv r_s/\sqrt{2}$)	13	11	mm
a : minor radius ($= r_s - r_0$)	5	4	mm
L : axial length	800	400	mm

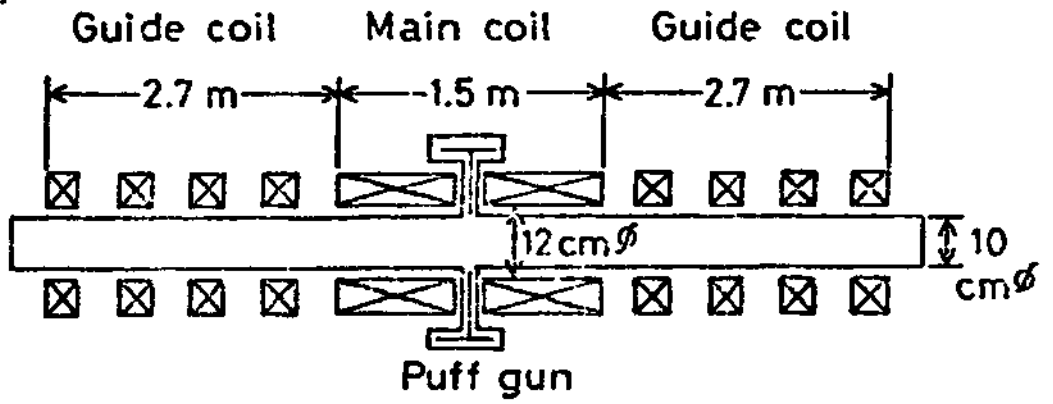
working gas : deuterium (D_2)

Table 1

	Ion	Electron
Thermal velocity (10^6 m/s)	$v_{th} \sim 0.18-0.14$	6.5
Larmor frequency (rad/s)	$\omega_i \sim 3.8-2.5(x10^7)$	$\omega_e \sim 1.4-1.0(x10^{11})$
Larmor radius (nm)	$\rho_i \sim 4.8-5.3$	$4.6-6.7(x10^{-2})$
Plasma frequency (rad/s)	$5.1x10^{10}$	$4.0x10^{12}$
Debye length (μ m)	1.0	
Collision time (s)	$\tau_{ii} \sim 1.2-0.7(x10^{-6})$	$\tau_{ei} \sim 3.8-5.3(x10^{-9})$
Collision frequency (1/s)	$0.8-1.4(x10^6)$	$2.6-1.9(x10^8)$
Mean free path (cm)	22-10	2.5-3.5
$\omega_i \tau_{ii}$	46-18	
$\omega_e \tau_{ei}$		540-510
r_s/ρ_i	3.1-2.7	

Table 2

(a)



(b)

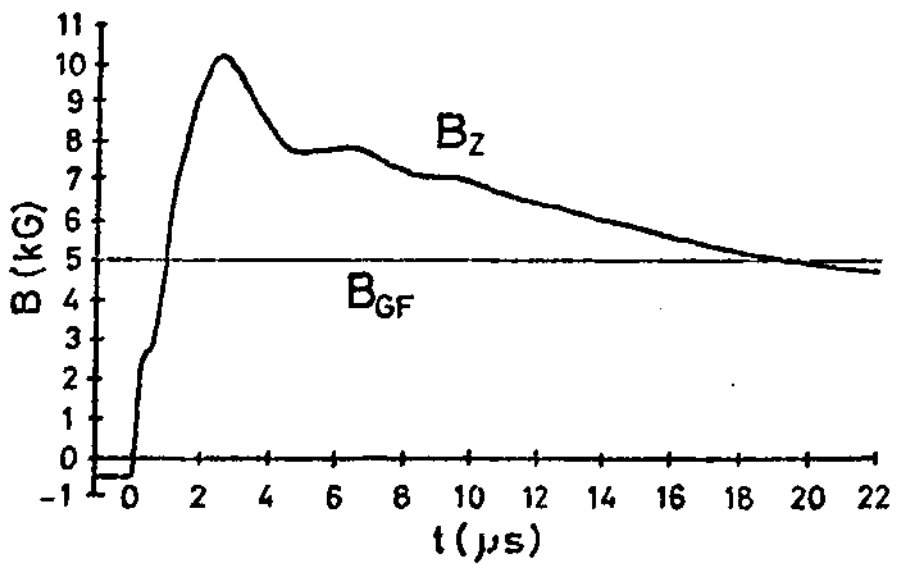


Fig. 1

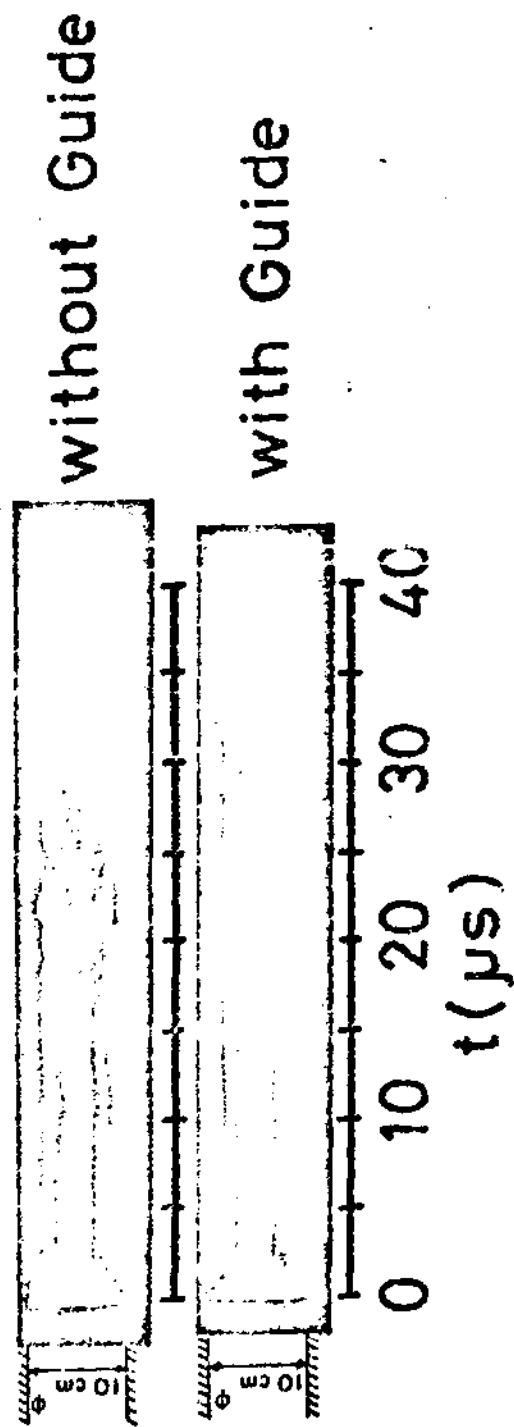


Fig. 2

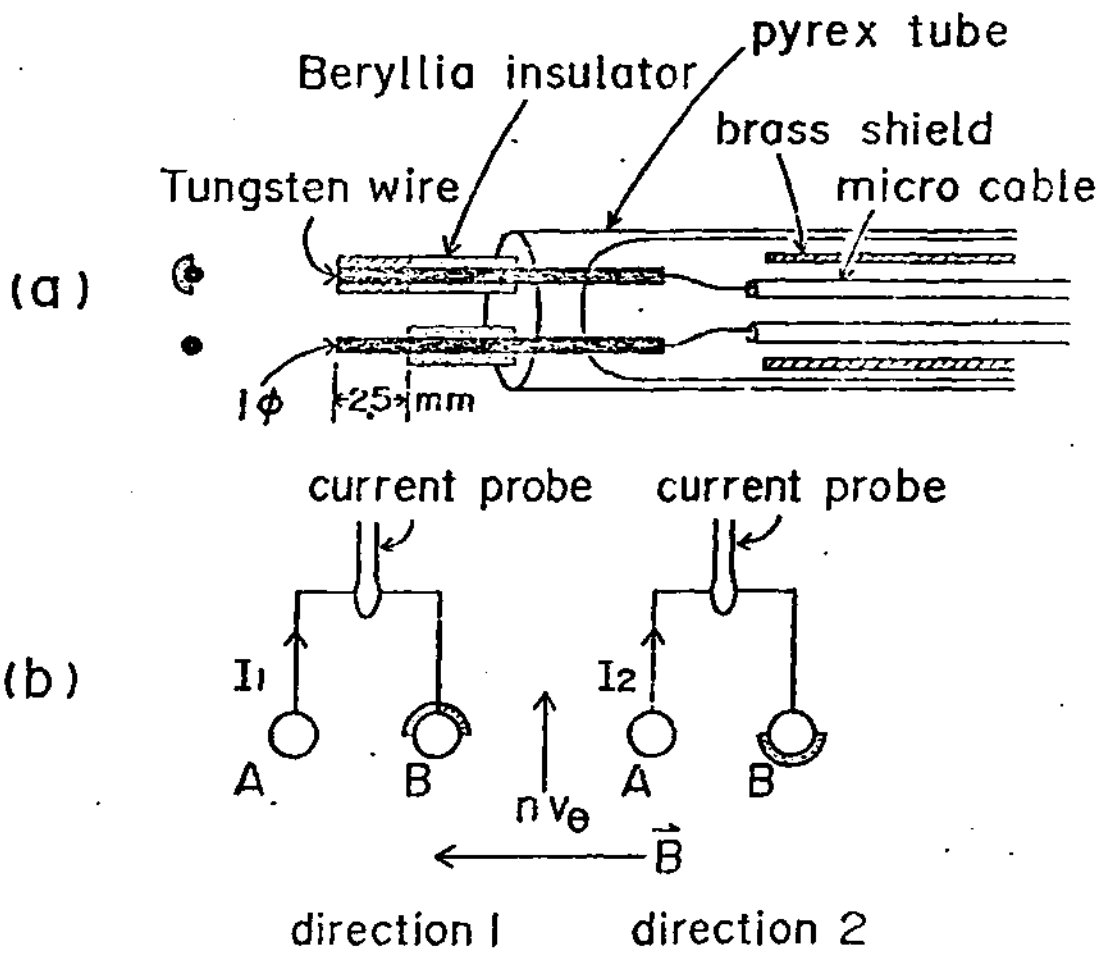


Fig. 3

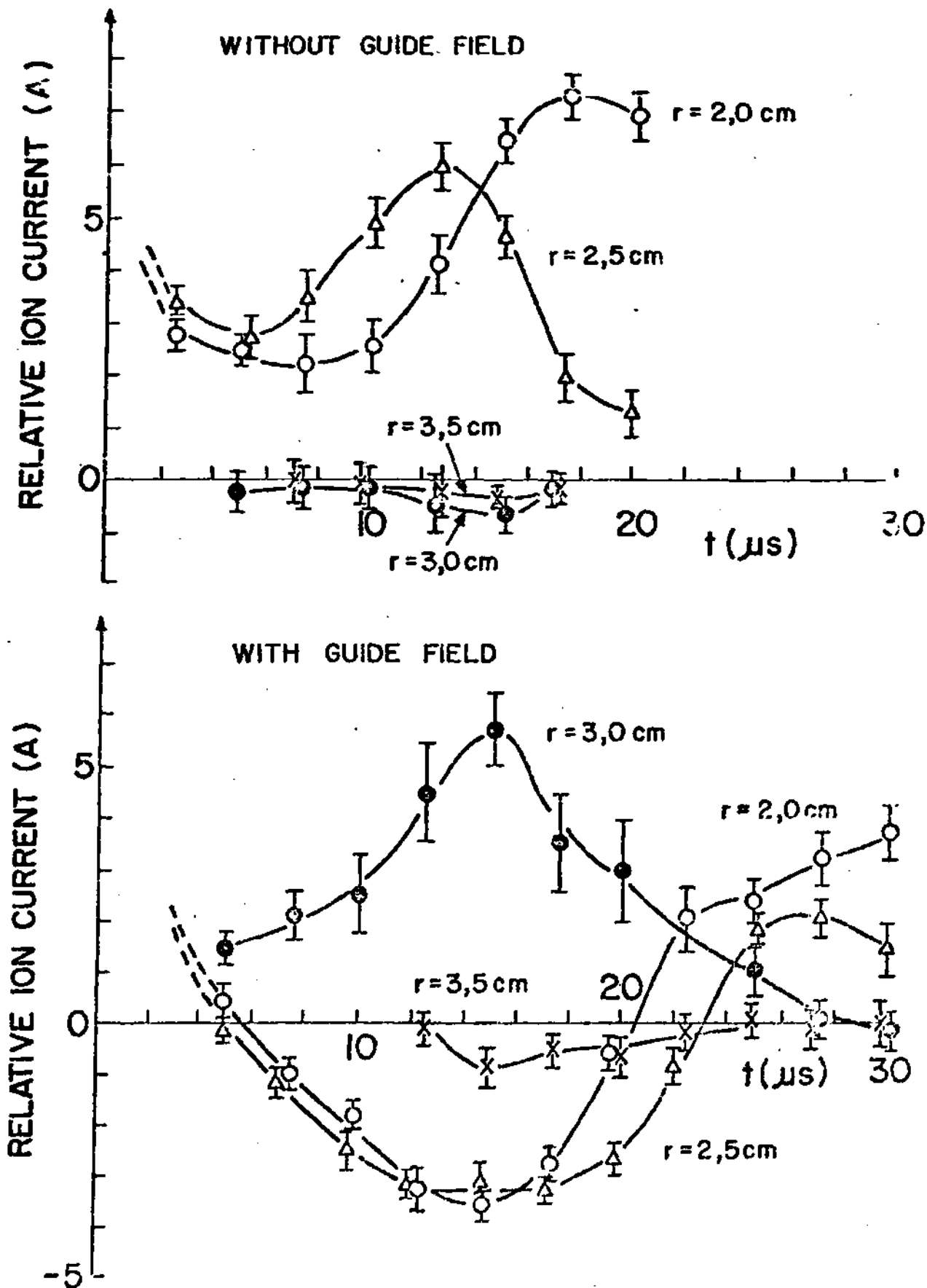
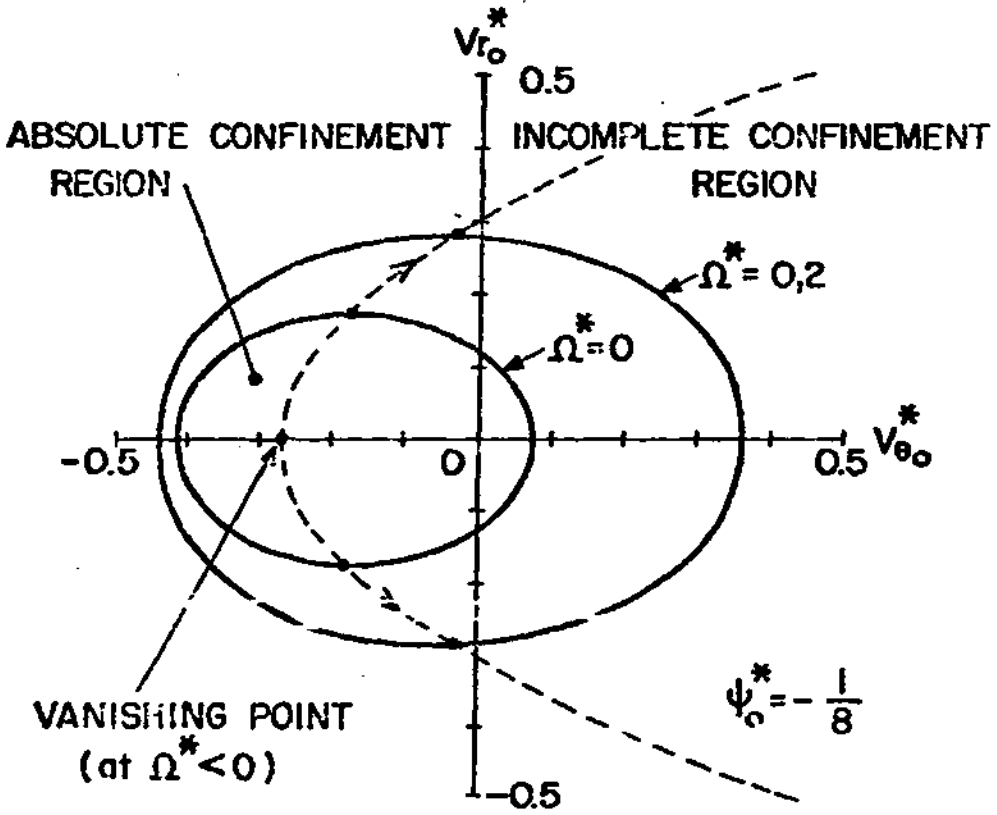


Fig. 4

a)



b)

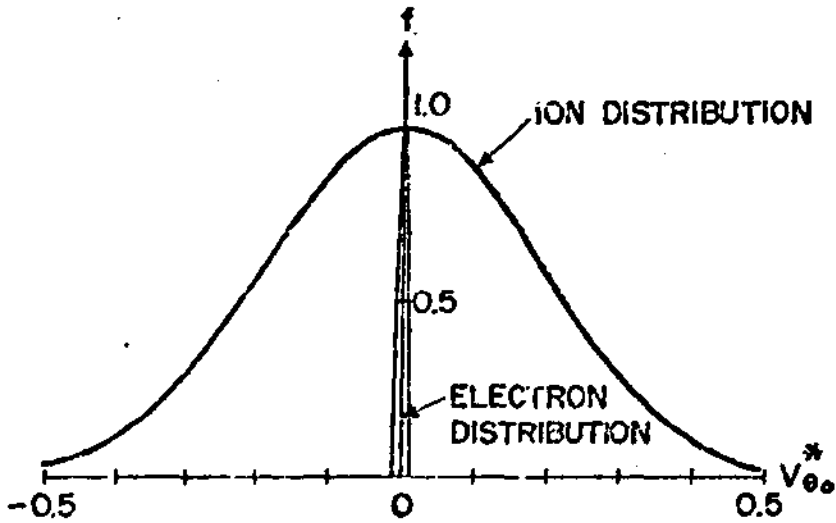


Fig. 5

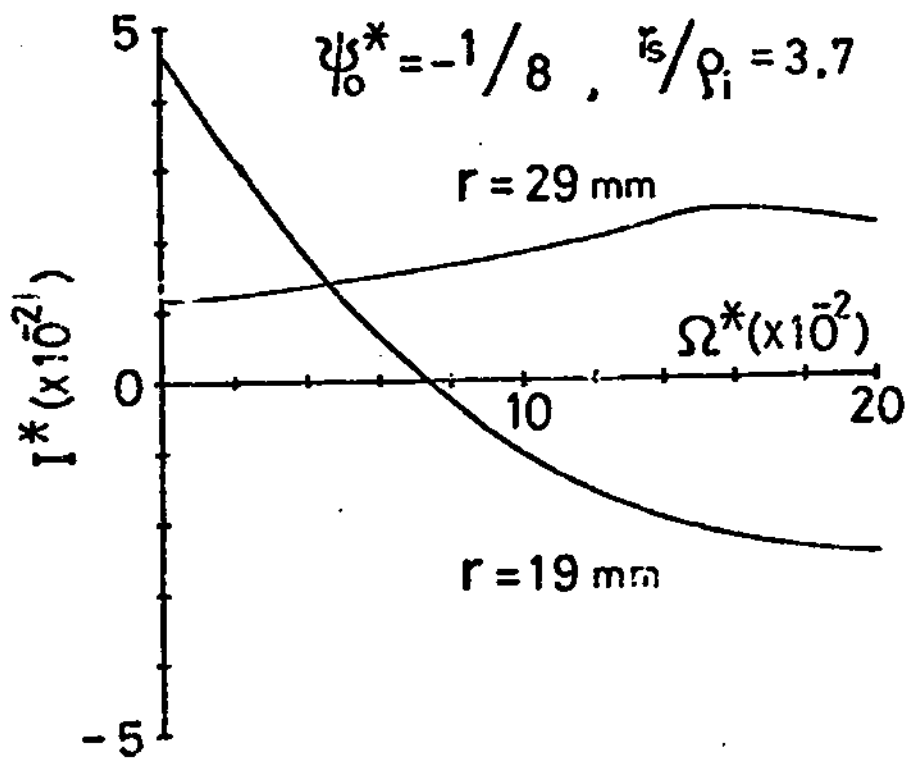


Fig. 6

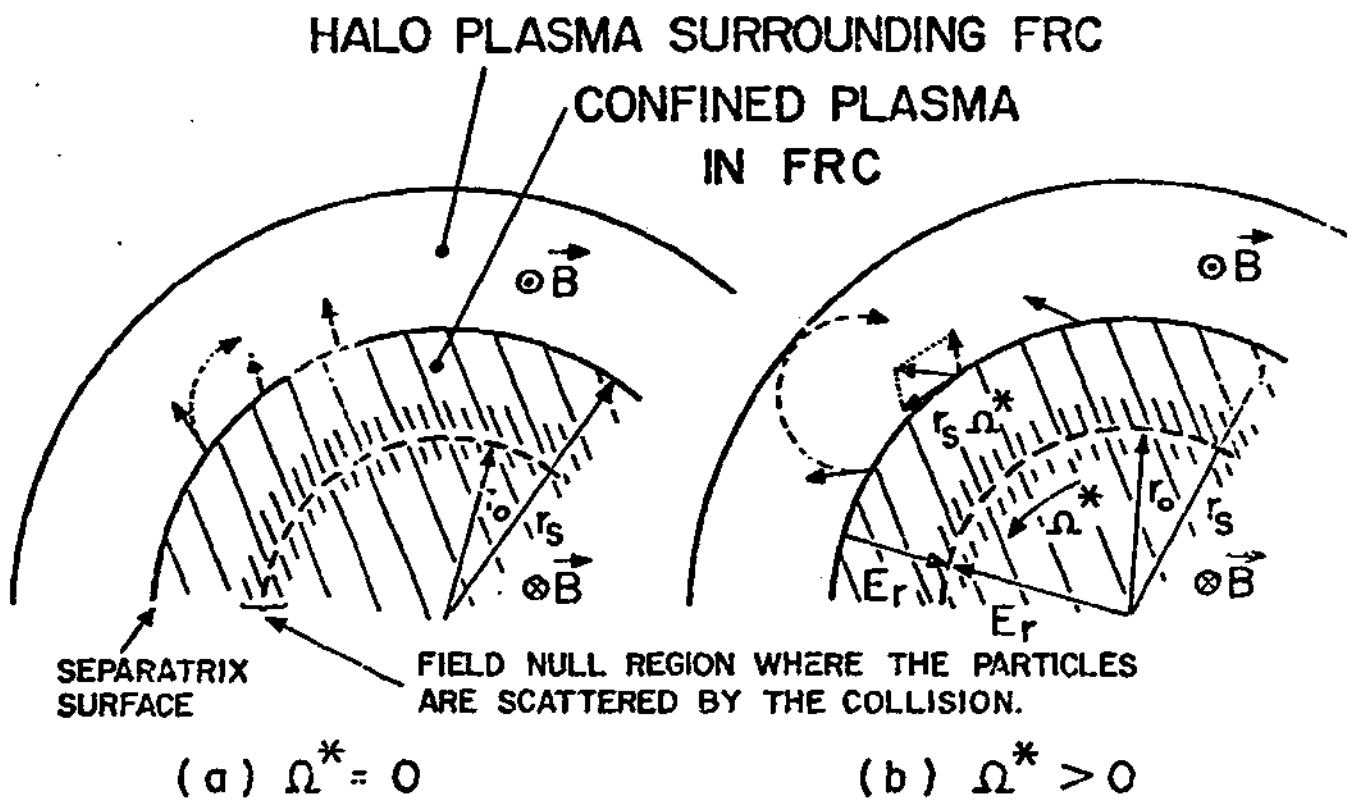


Fig. 7